Electronic Supplementary Material (ESI) for Dalton Transactions.


**Supporting Information**

# Heteroleptic naphthalo-phthalocyaninates of lutetium: synthesis and spectral and conductivity properties

Tatiana V. Dubinina,*[a,b] Anton D. Kosov,[a] Elizaveta F. Petrusevich,[a] Sergey S. Maklakov,[c] Nataliya E. Borisova,[a] Larisa G. Tomilova[a,b] and Nikolay S. Zefirov[a,b]

*[a] Chemistry Department, M.V. Lomonosov Moscow State University, 1 Leninskie Gory, 119991 Moscow, Russian Federation*
*Fax: +7 (495) 939 0290*
*E-mail: dubinina.t.vid@gmail.com*

*[b] Institute of Physiologically Active Compounds, Russian Academy of Sciences, 1 Severny proezd, 142432 Chernogolovka, Moscow Region, RussianFederation*
*Fax: +7-496-524-9508*
*E-mail: tom@org.chem.msu.ru*

*[c] Institute for Theoretical and Applied Electromagnetics, Russian Academy of Sciences, 125412, 13 Izhorskaya St., Moscow, Russian Federation*

**Contents list**

Table S1. High-resolution mass spectrometry MALDI TOF/TOF data.

| Compound (Molecular formula) | Mass found | Monoisotopic mass calculated |
|---|---|---|
| **3a** ($C_{128}H_{72}LuN_{16}$) | 2007.5519 | 2007.5534 |
| **3b** ($C_{128}H_{75}Cl_8LuN_{16}$) | 2290.1597 | 2290.3277 |
| **3c** ($C_{176}H_{105}LuN_{16}$) | 2616.8997 | 2616.8116 |
| **3d** ($C_{128}H_{73}LuN_{16}O_8$) | 2136.4387 | 2136.5205 |
| **3e** ($C_{128}H_{76}Cl_8LuN_{16}O_8$) | 2419.2322 | 2419.2943 |
| **3f** ($C_{176}H_{106}LuN_{16}O_{16}$) | 2873.7937 | 2873.7375 |

Table S2. $^1$H NMR data.

| Compound | $H_{Ph}$ (or $H_{PhO}$) | β-$H_{Pc}$ | β-$H_{Nc}$ | α-$H_{Pc}$ | α-$H_{Nc}$ | Solvent |
|---|---|---|---|---|---|---|
| **NcLuPc** [10] | - | 8.13 | 8.72 | 8.72 | 9.32 | [$D_6$]DMSO |
| **$^{Ph}$PcLu$^{Ph}$Pc** [4] | 7.35–7.43 | - | - | 9.02 | - | [$D_6$]DMSO–$CDCl_3$ (3:1, V/V) |
| **3a** | 7.40-7.56 | 8.17 | 8.72 | 8.81 | 9.42 | [$D_6$]DMSO |
| | 7.38-7.54 | 8.16 | 8.67 | 8.83 | 9.40 | [$D_6$]DMSO:$CDCl_3$ (3:1, V:V) |
| **3b** | 7.40-7.54 | - | 8.72 | 8.77 | 9.45 | [$D_6$]DMSO:$CDCl_3$ (3:1, V:V) |
| **3c** | 7.72-7.75 and 7.87-7.90 | - | 8.54 | 9.26 | 9.56 | [$D_6$]DMSO |
| **3d** | 7.18-7.28 and 7.44-7.50 | 7.94 | 8.08 | 8.81 | 9.15 | [$D_8$]THF |
| **3e** | 7.55-7.74 | - | 8.14 | 8.61-8.73 | 9.16 | [$D_6$]DMSO |
| **3f** | 7.51-7.59 and 7.67-7.75 | - | 8.15 | 8.17 | 9.27 | [$D_6$]DMSO |

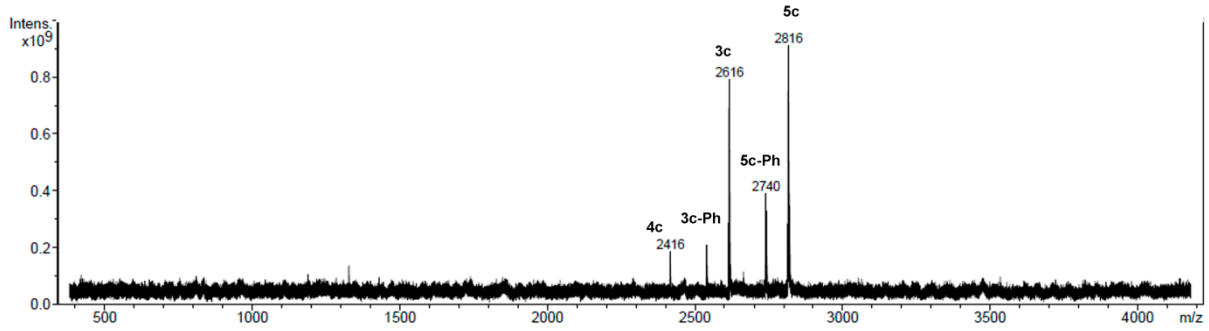


Figure S1. MALDI-TOF mass spectrum of a reaction mixture for synthesis of complex **3c**.

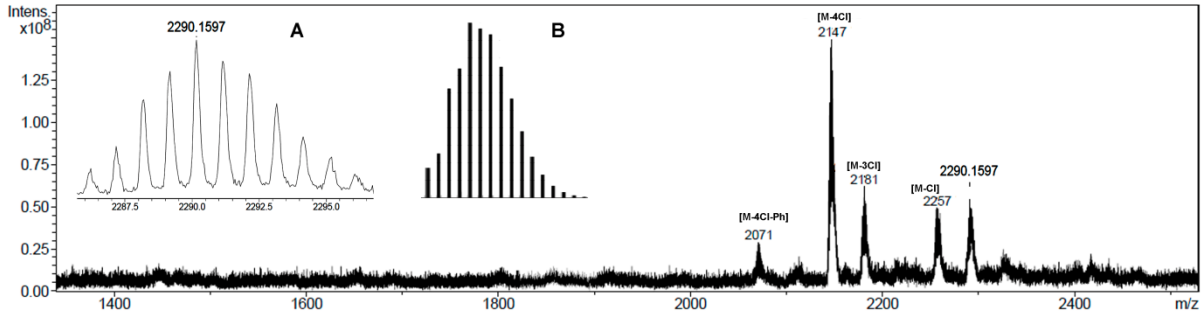


Figure S2. High-resolution MALDI-TOF/TOF mass spectrum of **3b**, isotopic patterns for the molecular ion (inset A) and simulated MS patterns of the molecular ion (inset B).

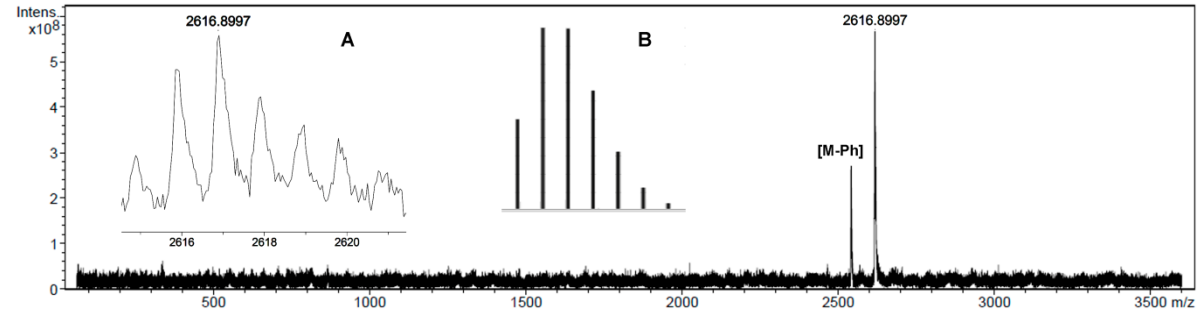


Figure S3. High-resolution MALDI-TOF/TOF mass spectrum of **3c**, isotopic patterns for the molecular ion (inset A) and simulated MS patterns of the molecular ion (inset B).

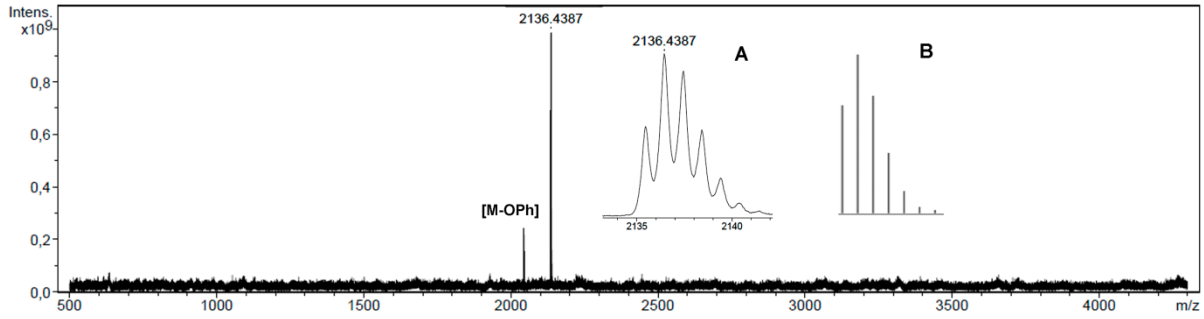


Figure S4. High-resolution MALDI-TOF/TOF mass spectrum of **3d**, isotopic patterns for the molecular ion (inset A) and simulated MS patterns of the molecular ion (inset B).

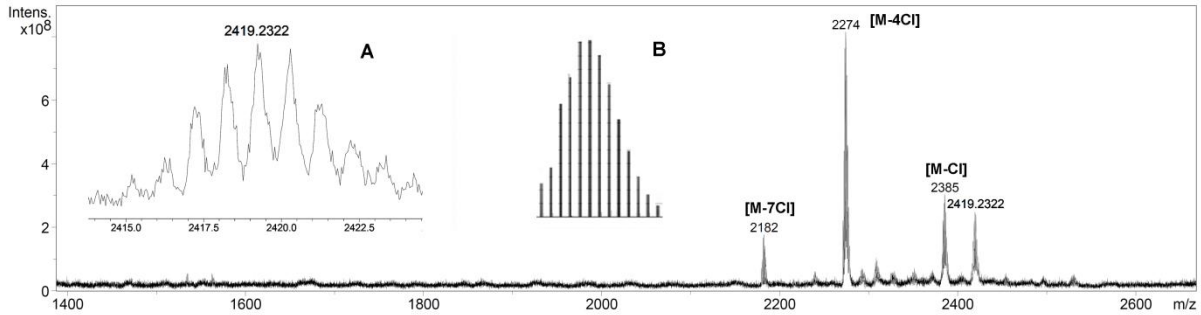


Figure S5. High-resolution MALDI-TOF/TOF mass spectrum of **3e**, isotopic patterns for the molecular ion (inset A) and simulated MS patterns of the molecular ion (inset B).

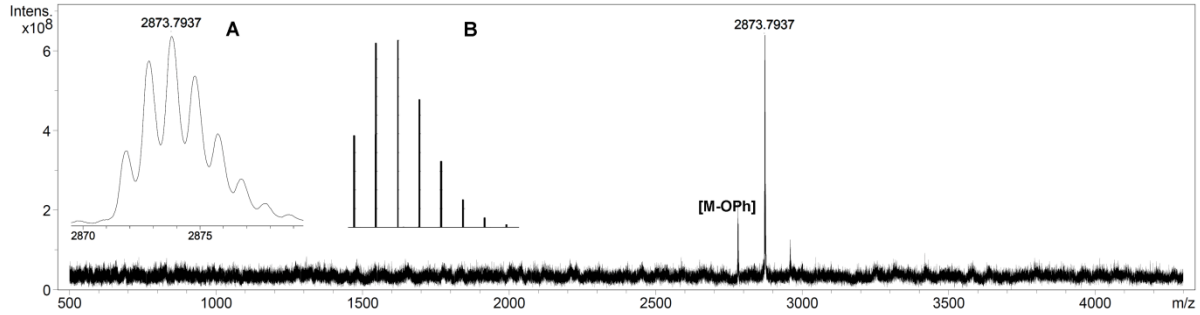


Figure S6. High-resolution MALDI-TOF/TOF mass spectrum of **3f**, isotopic patterns for the molecular ion (inset A) and simulated MS patterns of the molecular ion (inset B).

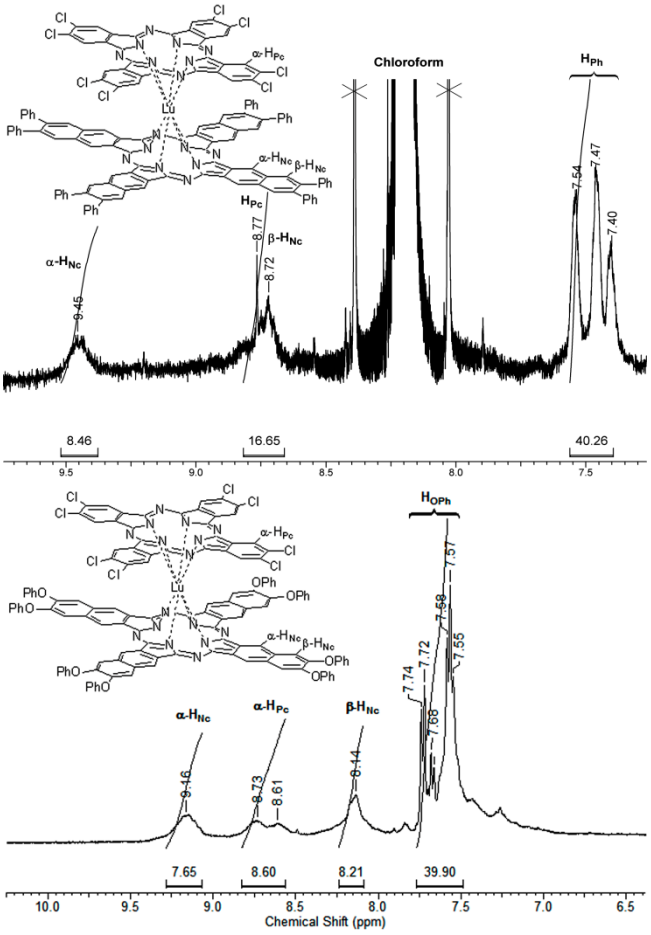


Figure S7. $^{1}$H NMR spectra of complexes **3b** and **3e**.

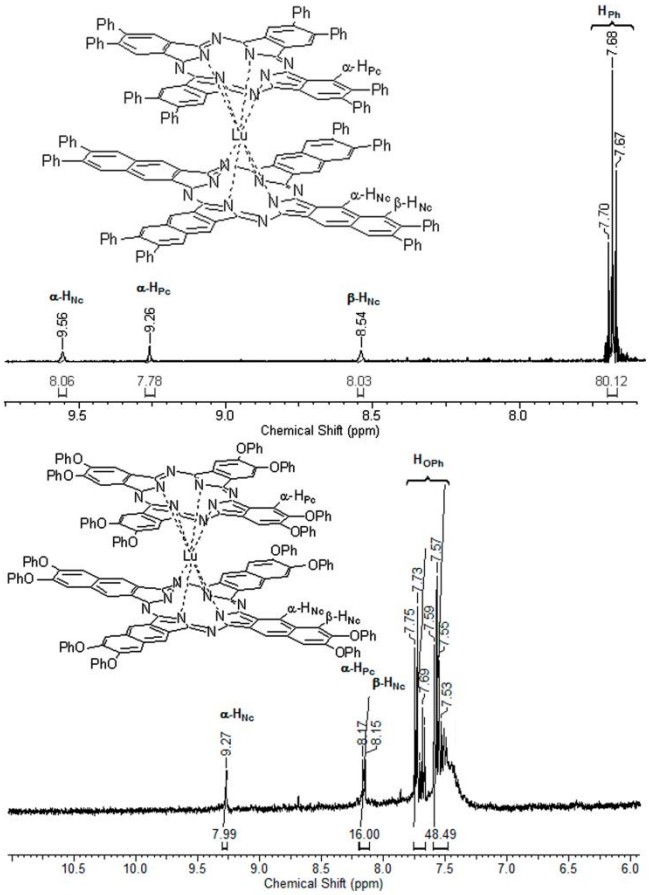


Figure S8. $^{1}$H NMR spectra of complexes **3c** and **3f**.

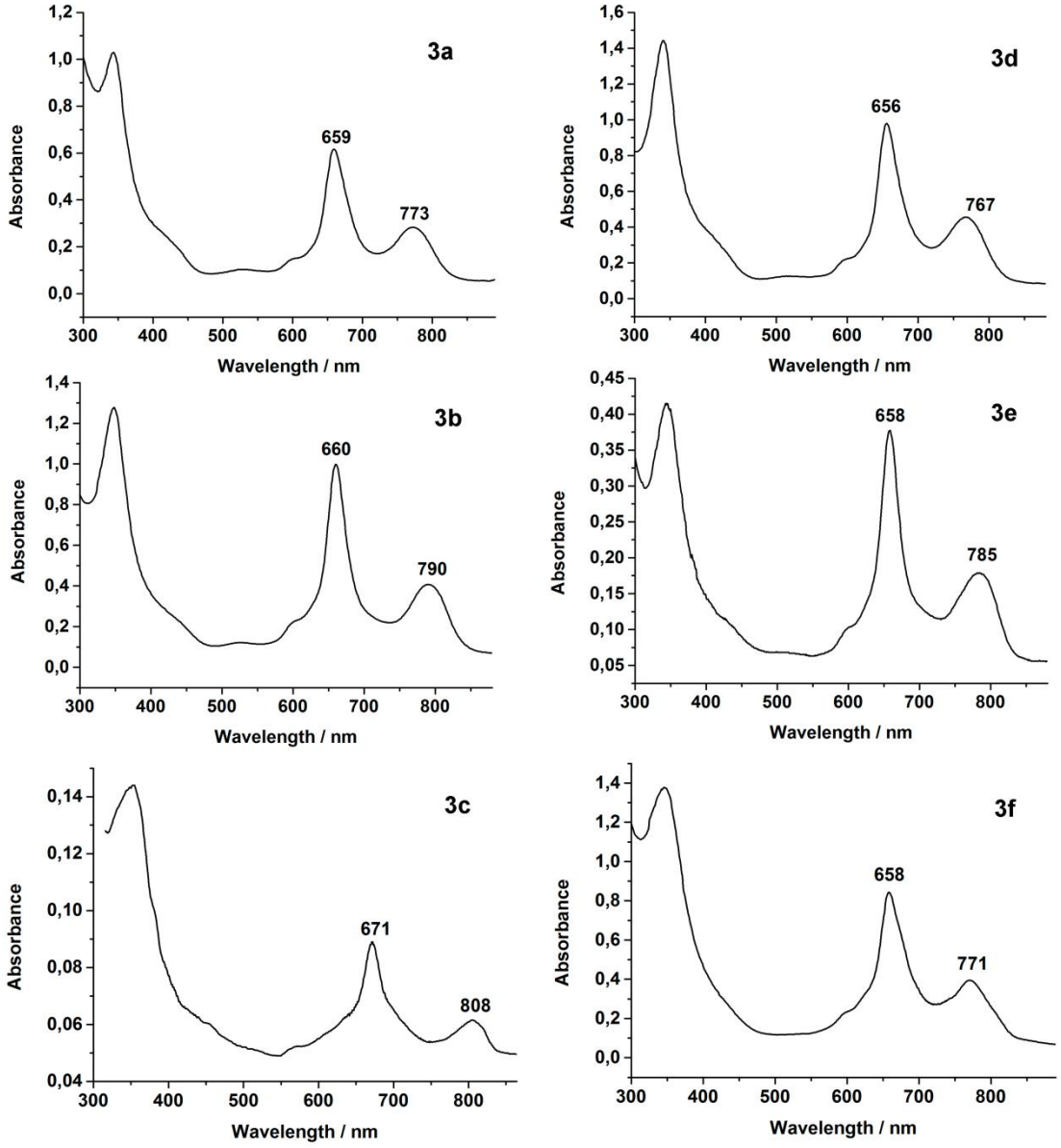


Figure S9. UV-Vis spectra of reduced by $N_2H_4 \bullet H_2O$ forms of heteroleptic complexes **3** in DMSO.

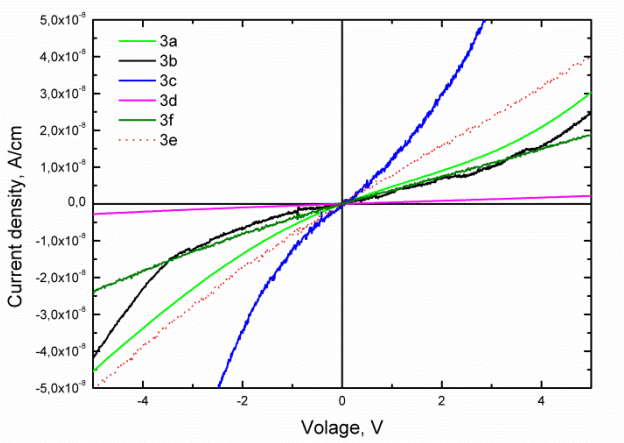


Figure S10. I-V curves for thin films of heteroleptic complexes **3**.

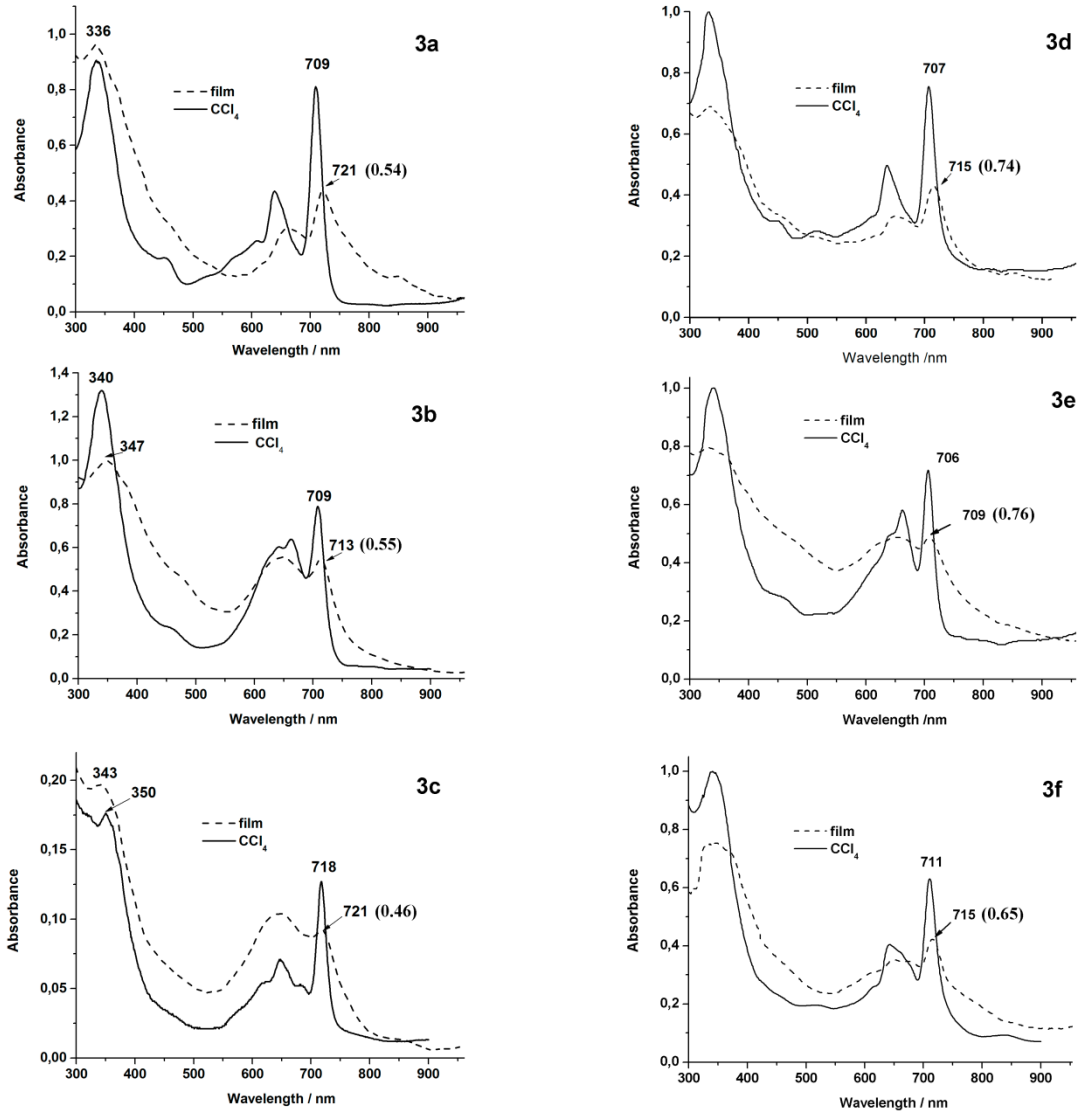


Figure S11. UV-Vis spectra of thin films and solutions in $CCl_4$ for heteroleptic complexes **3**. The Q-band:B-band intensity ratios for thin films are given in brackets.

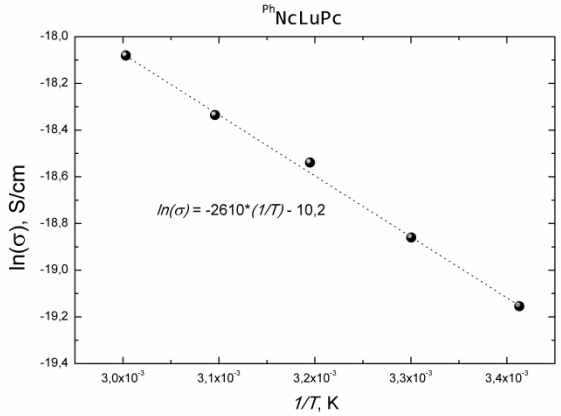


Figure S12. Conductivity of a thin film of complex **3a** as a function of temperature (ln(σ) vs. l/T).

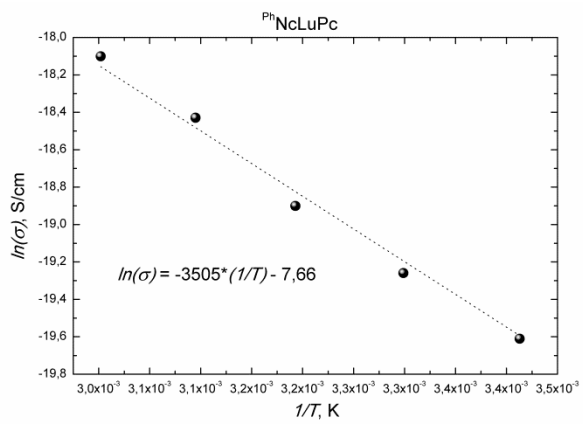


Figure S13. Conductivity of a thin film of complex **3b** as a function of temperature (ln(σ) vs. l/T).

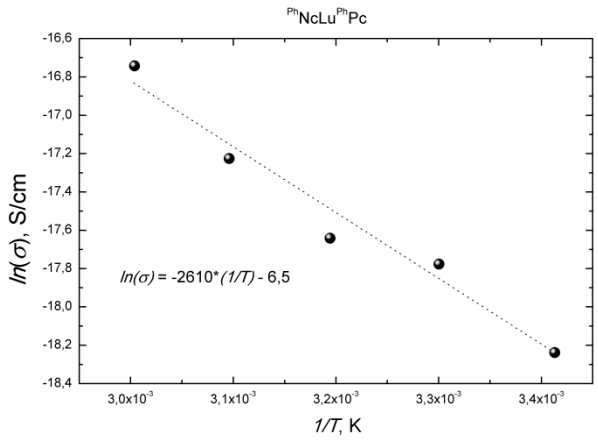


Figure S14. Conductivity of a thin film of complex **3c** as a function of temperature (ln(σ) vs. l/T).

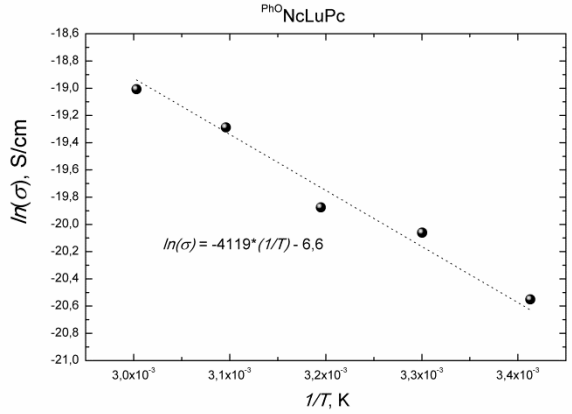


Figure S15. Conductivity of a thin film of complex **3d** as a function of temperature (ln(σ) vs. l/T).

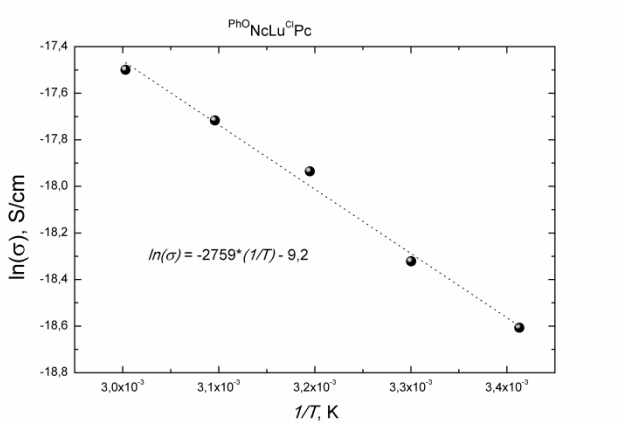


Figure S16. Conductivity of a thin film of complex **3e** as a function of temperature (ln(σ) vs. l/T).

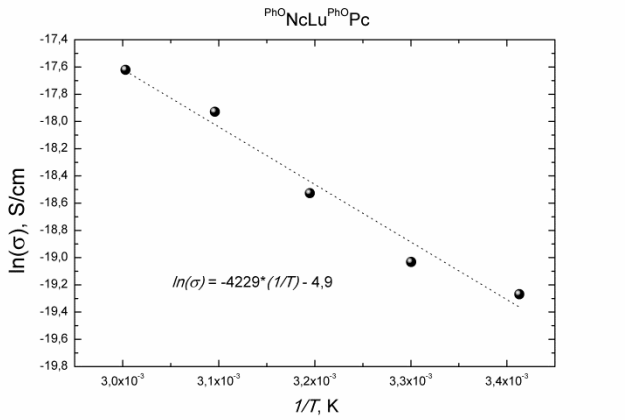


Figure S17. Conductivity of a thin film of complex **3f** as a function of temperature (ln(σ) vs. l/T).

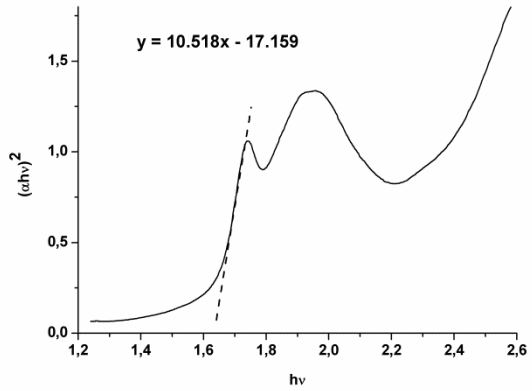


Figure S18. Tauc plot for the Q-band of the thin film of phthalocyanine **3b**.

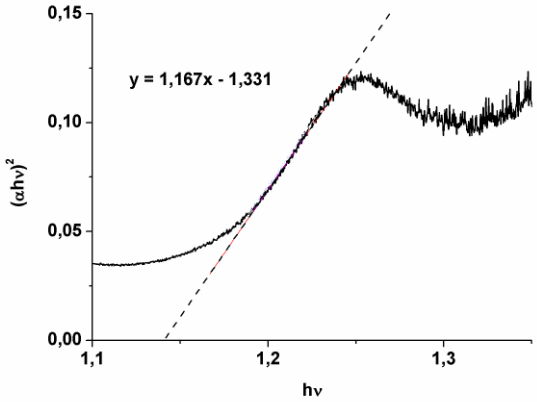


Figure S19. Tauc plot for the RV-band of phthalocyanine **3b**.